A Novel Saliency Region Enhanced Technique for Biomedical Image Indexing Using Deep Learning

Pradeep Kumar Jena[1], Bonomali Khuntia[2*], Trilochan Panigrahi[3]

[1] Department of Computer Science and Engineering, NIST Institute of Science and Technology, Berhampur 761008, India
[2] Department of Computer Science, Berhampur University, Berhampur 760007, India
[3] Department of ECE, National Institute of Technology, Goa 403401, India

Corresponding Author Email: bonomalikhuntia@gmail.com

ABSTRACT

Today's advanced medical facilities have created a space for a better understanding of many health-related issues such as fractures, tumors, infections, etc. through augmented digital imaging. High-quality medical imaging technologies, which includes Magnetic Resonance Imaging (MRI), Positron Emission Tomography (PET), Computerized Tomography (CT) scans, and X-rays, has enriched our understanding of various health ailments such as fractures, tumors, and infections. These imaging techniques provide a considerable advantage in early disease detection by analysing visual cues. The objective of this work is to find the Region-of Attention (RoA) or the saliency region of an image using deep learning i.e., U-Net for precise RoA segmentation. The saliency region is enhanced and fused with the original image to generate a new enhanced image. The CNN features of this enhanced image are used for the similarity finding and image indexing. In this work a novel framework, termed Saliency-Region Enhanced Content-Based Image Retrieval (SRE-CBIR) is proposed. The efficacy of the SRE-CBIR model was tested on two biomedical image datasets, specifically, Brain tumor and COVID-19 datasets. The classification results show there are enhancements in the No-tumor and Covid-negative cases. The average precision value of original Brain tumor dataset is 94.3% where as it is 95.0% for the enhanced Brain tumor dataset, likewise the average precision value of original COVID19 dataset is 97.0%, which is 98.0% when tested for the enhanced COVID19 dataset. Retrieval results using CNN features of the enhanced images outperform the retrieval of the CNN features of the original images in terms of class-wise as well as the average retrieval rate.

1. INTRODUCTION

The case-based analysis is a common practice for medicine experts. Finding the information of previous patients helps the doctor with additional support for better understanding of critical cases and proper diagnosis [1]. Content based medical image retrieval (CBMIR) system used to retrieve the images of similar cases from the large medical image database [2, 3]. The content refers to the visual image features derived from the textures, colors, shapes [4-7] etc. The feature matching exhibits visual similarities, which is based on similarity extracted features rather than the exact matching. The retrieval results are then ranked accordingly to their similarity index [8-10]. Medical image analysis is cumbersome since radiological images are high-resolution images. Moreover, finding the image features which are really meaningful for a radiologist is also challenging. Hence building a CBMIR system is a more tedious task than the CBIR system. Manual annotation of medical images with precise descriptions or labels is no longer possible due to its exponential growth, multimodal nature [11, 12], and lack of properly defined standards.

Traditionally handcrafted features are also not very useful

due to its high resolution and complex possessions. The major challenges in medical image analysis are first most of the radiological imaging are gray-scale and multi-modal in nature, i.e. the X-rays images are used for detection of (a) bone fracture analysis (b) the chest X-rays are used for the diagnosis of COVID-19 and pneumonia [13-18] analysis (c) in case of Mammogram the X-rays image is used for breast cancer detection [19]. Likewise, the computed tomography (CT) scan image shows a detailed view of the bones, tissues and other organs inside the body [20]. The X-ray and CT scan images are also used for the Brain tumor detection [21-23]. In the case of a high resolution computed tomography (HRCT) scanning the slices are much thinner than that of a standard CT scan, so it gives a more comprehensive view of the chest. It maps the three-dimensional (3D) to a cross-sectional view in two-dimensional (2D) called "slice" [24]. Images produced by Magnetic resonance imaging (MRI) scan [25] are useful to understand the different abnormal conditions of the chest, abdomen and brain. Hence retrieving similar images from multiple modalities is more challenging. Second, the limited number of pathological information available for many critical cases. With the availability of high-speed computing facilities using GPUs and TPUs and the evolution of Deep learning

techniques, medical image analysis has become a more focused research domain. Computer-aided diagnosis (CAD) [26] models are developed to automate the diagnosis process. Deep learning is used for automatic medical image segmentation, i.e. to find the region-of-interest [27, 28] as well as for image classification using the Convolutional neural network (CNN) feature [29-34]. An efficient image retrieval system can be helpful for the automation of medical data management in hospitals. It will assist the physician for faster decision making by reviewing the previously available clinical cases [35-38]. The service can be extended to the remote health centers to support the newly appointed doctors as a cloud based service.

In this work our objective is to develop a more effective CBMIR system using CNN feature of the enhanced medical images. The CNN feature extraction uses the Max-pooling operation after each convolution operation, so the CNN feature of the enhanced image is expected to be a better image descriptor than the CNN feature of the original image. First the medical images are segmented using deep learning (U-Net) [39, 40] to find the region-of-attention i.e. the target region of a biomedical image according to their image class. Here the RoA segmented image is referred as mask image. Then the segmented images are enhanced. These enhanced segmented images are fused with its original image to produce a complete enhanced image. The proposed CBMIR system for the biomedical image analysis and retrieval is developed and tested using two publicly available biomedical image datasets i.e. Brain tumor dataset, it consists of four classes and Covid-19 dataset which consists of three classes. The classification and retrieval performances of both the datasets are presented in the result section.

The major achievements of the proposed method are:

• The deep learning technique is applied to extract the RoA as per the class of the radiological image.

• The RoA image is enhancement is done using Contrast-limited adaptive histogram equalization (CLAHE).

• The enhanced RoA image is fused with the input image to generate a complete enhanced image.

• CNN features of the fused enhanced image are used as the image descriptor.

• A CBIR model is developed and tested with two publicly available biomedical image dataset i.e. Brain tumor and COVID19 dataset.

• The performance retrieval performance of the original image and enhanced image datasets are compared.

The rest part of this paper is arranged as per the following order: Section 2 shows a review of medical image analysis and the CBIR system. Section 3 presents the proposed RoA segmentation technique using U-Net, the image enhancement and the CNN feature extraction. Section 4 shows the detailed classification and retrieval results. Section 5 presents the conclusion and future scope of the work.

2. LITERATURE SURVEY

Kim et al. [2] proposed a region-based query model for the medical image a retrieval. Here the volume of interest (VOI) is based on the content-based retrieval of four-dimensional i.e. three spatial and one temporal domain features of the positron emission tomography (PET) images are employed for this purpose. It is used to retrieve the image with similar visual,

and functional VOI features. Devulapalli et al. [5] developed a CAD system for medical image analysis using a hybrid feature descriptor. The hybrid feature is generated by combining the deep-learning Googlenet feature with the Gabor texture features and its performance is explored for the retrieval of medical images. Pang et al. [8] proposed an efficient image indexing and retrieval method by using deep learning and the preference learning technologies for the biomedical image retrieval. The authors claim its result is more accurate for discriminative image retrieval. Majhi et al. [9] developed an image retrieval technique based on the encrypted feature where the luminance and chrominance features are extracted in two different phases.

Euclidean distance is used to measure the similarity of the encrypted feature of two different images. Horry et al. [11] suggested transferred learning CNN model for the COVID-19 detection. The detection of COVID-19 with respect to pneumonia or normal for three different modality lung images i.e. X-Ray, Ultrasound CT scans images are tested through Transfer Learning using VGG19 model, which is a deep-learning neural network model comprising of 16 convolution layers and 3 fully connected layers. Here the results of the Ultrasound scanned image outperform the others. Kurian et al. [12] proposed a Multimodality medical image retrieval using CNN. Here the authors used medical images of seven different modalities. They also explored the performances of different optimizers such as Adam, SGD and AdaGrad of deep learning. Abbas et al. [13] developed a deep CNN model using Decompose, Transfer, and Compose and they referred it as (DeTraC) used for COVID-19 classification using chest X-ray images. The proposed model is validated with different pre-trained CNN models and the author cited highest accuracy has been achieved using VGG19 network. Nayak et al. [17] evaluated the performance of eight pre-trained Convolutional Neural Network (CNN) models such as VGG-16, GoogleNet, AlexNet, MobileNet, ResNet, and SqueezeNet, for classification of COVID-19 using the X-ray images of chest also compare the performances for different parameters such as learning rate, number of epochs, batch size and type of optimizers. Pathan et al. [20] introduces an optimized CNN-based architecture for the precise recognition of COVID-19 from the CT scan images. Here the WOA-BAT techniques are ensembled to optimize CNN parameters.

Saba et al. [21] suggested a Brain tumor detection framework using fusion of hand crafted with deep learning features. The Brain tumor images are first segmented to identify the actual lesion region, then the hand crafted and deep learning features are extracted from the segmented images. It is claimed that the features can be used for the multimodal Brain tumor dataset. Mudda et al. [22] presented a Brain tumor classification model with statistical features i.e. the texture feature. In this the Edge-based Contourlet Transformation is used for multiple input image registration and fusion. The Region of Interest (ROI) i.e. tumor region is segmented to provide accurate boundaries. Then the Gray-Level Run Length Matrix (GLRLM) and Center-Symmetric LBP(CSLBP) texture features are fused and the classification is done using ANN. Mukkapati and Anbarasi [26] proposed a Brain tumor segmentation using U-Net, here they have used RefineNet for pattern analysis and SegNet for classifying Brain tumor image. They have used bench-marked Brain tumor dataset to analyze the efficiency of their proposed enhanced CNN model. Authors claim U-Net provides better segmentation with respect to the local as well as the context

MRI image information. The SegNet is useful for the precise features extraction and classification.

Authors of this system will be helpful for the analysis of radiological image. Pradhan et al. [27] proposed a CBIR framework using region based feature extraction and fusion. Here the RoA of a given image is identified and the multi-directional texture features, and correlation-based spatial color features are extracted and fused to define a better image descriptor. The model performance is tested with five different datasets. Lai et al. [32] presented a medical image classification algorithm by combining the high-level medical image features with traditional image features to enhance medical image classification. Öztürk [33] developed a CBMIR framework using high-level deep features to minimize the semantic gap within the low-level medical image features and the high-level visual features by producing the more effective and minimal parameterized hash codes using the deep learning features of the image. The detailed survey of medical image analysis is presented in Table 1.

Table 1. Survey table of medical image analysis

Sl. No.	Research Study/ Year	Method Used	Modality of Scan	Image Database
1	Horry et al. [11]	Deep Learning VGG19.	Chest X-ray	COVID19
2	Ismael et al. [16]	Deep Learning ResNet50 Features with SVM.	Chest X-ray	COVID19
3	Pathan et al. [20]	CNN hyperparameters are optimized using WOA-BAT optimization techniques.	Chest CT-Scan	COVID19
4	Deepak et al. [25]	Deep Learning pre-trained GoogLeNet.	Brain Tumor MRI scan	Brain MRI
5	Pradhan et al. [27]	RoA based feature extraction and fusion.	-	Corel, GHIM
6	Panwar et al. [35]	Deep Learning nCOVnet.	Chest X-ray	COVID19

3. PROPOSED METHOD

In this work, a novel enhanced saliency region based CBIR model is proposed for the medical image retrieval. Here the CNN features are used as the image descriptor, which is used for finding the similarity indexes between the query image and the images in the database. Most of the medical images are high-resolution images and the doctor's attention goes to only the region of ailment i.e. the RoA region. Many cases these RoA regions are less prominent in the original image. The factual features available in the less prominent RoA region of an image are suppressed by the MAX-pool operation during CNN feature extraction as the MAX-pool is applied recursively with each convolution operation [39]. The objective of this work is to enhance the RoA before feature extraction to derive a better image descriptor as the image class. Figure 1 shows the U-Net architecture used for segmentation of the RoA i.e. to generate the mask image as per their class information using supervised learning technique [40].

Figure 1. U-Net architecture for masked-image generation

Figure 2 shows the model for the proposed CBIR system, here medical images are segmented using deep-learning. Where the segmented masks are enhanced using CLAHE and fused with the original image to produce final enhanced image, and are used for the CNN feature extraction [37]. The Table 2 shows the saliency region enhanced image with the original image and the mask-image of the Brain tumor and COVID19 dataset [36, 38]. The City-block distance measure is used for finding the similarity index between the query image and the images in the database. The performance of the proposed model is presented using precision, recall, f1-score, ROC analysis and retrieval rate for both the above mentioned datasets.
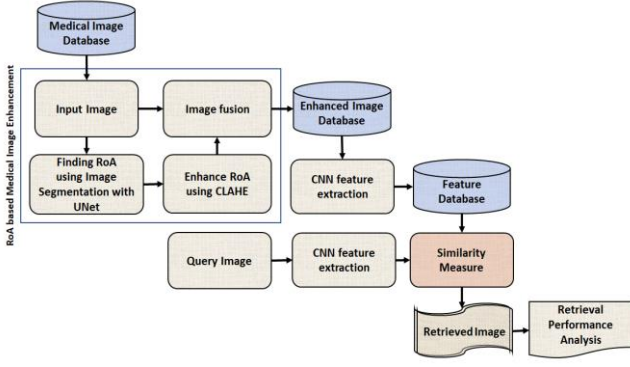
Table 2. Saliency region enhanced images

Figure 2. Proposed SRE-CBIR model

3.1 CNN feature extraction

The proposed model illustrated in Figure 1 shows the CNN features of the enhanced medical images are generated. Here the gray-scale image is resized to 512 x 512, which is given to the CNN model for training. The proposed CNN model contains of seven layers, here each layer consists a convolution, which is followed by the ReLU and then a MAX pool operation. The activation function ReLU introduces non-linearity property to the convolution output. The image size is reduced by the MAX pooling operation with each convolution layer. The image is reduced to a 1D feature vector of 1 x 1024 by the flattened layer. Four fully connected layers are used for additional dimensional reduction. Soft-max operation converts the feature map to class label using the energy function [6].

$$(I * f)_{x,y} = \sum_{s=1}^{H} \sum_{t=1}^{W} f_{s,t} \cdot I_{x+s-1,y+t-1} + b \qquad (1)$$

$$ReLU(x) = Max(0, x) \qquad (2)$$

$$E(w, b) = \frac{1}{n} \sum_{i=1}^{n} L(y_i, f(x_i)) + \alpha R(w) \qquad (3)$$

where, L: The loss value of the model; R: The regularization factor used to deal model complexity; α: strength control value of the regularization value.

The precision value represents the number of images rightly recognized by the system with respect to the number of image recognized by the system. Whereas the recall value indicates the number of images correctly recognized to a given class with respect to number of images available in the database for the same class. So the value of average recall rate is a more significant measuring parameter in case of retrieval analysis. The harmonic mean of all the classes is presented using f1-score.

$$S_i(x) = \frac{1}{1+e^{-x}} \qquad (4)$$

$$LogLoss = -\frac{1}{N} \sum_{i=1}^{N} \sum_{j=1}^{M} y_{ij} log P_{ij} \qquad (5)$$

The convolution operation at a point a (x, y) is represented in Eq. (1). Here the I represent a gray-image and the f is the operational filter, here H is the height and W is the width of the image. The ReLU operation is defined in Eq. (2). The Eq. (3) represents regularized training error of an instance. The S_i is the sigmoid function that maps the output value within (0,

1) is defined in Eq. (4). The penalty value for each iteration is represented using Eq. (5) i.e. cross-entropy loss using the energy function [6].

3.2 Performance measures

The efficacy of the proposed SRE-CBIR model is measured using quantifier parameters such as precision, f1-score, and recall these are defined using Eq. (6), Eq. (7), and Eq. (8) respectively [26].

$$Precision = \frac{True+ve}{True+ve+False+ve} \qquad (6)$$

$$Recall = \frac{True+ve}{True-ve+False-ve} \qquad (7)$$

$$f1 - Score = 2 \times \frac{Precision \times Recall}{Precision+Recall} \qquad (8)$$

here, *true +ve* value represents the total number images correctly recognized by the system to their belonging class. The *false -ve* value indicates number of images wrongly identified by the system for a particular class, and the *false -ve* value shows number of images rejected by the system falsely.

Receiver operating characteristics (ROC) is the curve shows the stability of the model, it is plotted using the values of *true+ rate* vs *false- rate* [26]. The City-block distance used to measure the similarity index value between the query image and the database image is shown in the Eq. (9).

City-block distance measure:

$$D_{CT} = \sum_{i=0}^{L-1} |F_i^q - F_i^t| \qquad (9)$$

where, F_i^q: feature vector of the query image; F_i^t: feature vector of the database image.

4. RESULTS AND DISCUSSION

The proposed SRE-CBIR system performances for medical image retrieval is presented in this section. In the first stage the RoA of the radiological image is segmented using U-Net, which is a deep learning method. The segmented using U-Net, which is a deep learning method. The segmented RoA image is referred to as the mask-image which is automatically identified using supervised learning. Then mask-image is enhanced applying CLAHE to support better CNN feature generation. Finally the enhanced mask-image is fused with the rest part of the input image and generates the new complete enhanced image. A better CBIR model is developed using the CNN features of the enhanced image database. The classification and retrieval performance using enhanced image are tested with two medical image datasets i.e. Brain tumor dataset having a total 3160 images of four classes and the COVID19 dataset having 6498 images of three different classes.

4.1 Results analysis of Brain tumor

Table 3 shows the results of the Brain tumor dataset, the average precision using original BT image is 94.3%, which is 95.0% using the enhanced BT image. Result shows the weighted average precision is also increased by .5%.

Table 3. Performance analysis of Brain tumor dataset

	Original BT Image			Enhanced BT Image			
	Precision	Recall	f1- Score	Precision	Recall	f1-Score	Support
No Tumor	0.92	0.95	0.94	0.94	0.96	0.95	396
Glioma	0.95	0.94	0.95	0.97	0.95	0.97	926
Meningioma	0.93	0.93	0.92	0.91	0.92	0.92	937
Pituitary	0.97	0.96	0.96	0.98	0.97	0.97	901
Macro Avg.	0.943	0.945	0.943	0.950	0.950	0.953	3160
Weighted Avg.	0.946	0.944	0.943	0.951	0.948	0.953	3160

The precision value is enhanced for all other classes except the Meningioma class which is 93% with the original image and 91% with enhanced image. The average recall rate is improved from 94.5% to 95% and the f1-score is increased from 94.3% to 95.3% using enhanced image dataset. Total 3160 images of four classes are analyzed and the number of images belonging to different classes are shown as the support value.

Figure 3 shows the ROC analysis of the original and the enhanced Brain tumor image. There is minor discernment in the ROC results of the Glioma and the Meningioma tumor classes, however the macro-average ROC is enhanced from 98% to 99% using the proposed enhancement method.

Figure 4 shows the top 20 retrieved Brain tumor images with respect to a query image. The query image is shown using a green border, whereas the image in a red border implies falsely retrieved other class images. The assessment of the class-specific retrieval performances for the top 10 Brain tumor images are shown in Figure 5. The performances of all the classes except the Meningioma class are comparatively enhanced using the proposed SRE-CBIR model. Figure 6 presents the average retrieval rate of the top 40 Brain tumor images. This shows that the average rate of retrieval performance improves as more images are retrieved. This result ascertains more class information is retained using the CNN feature of the enhanced BT images.
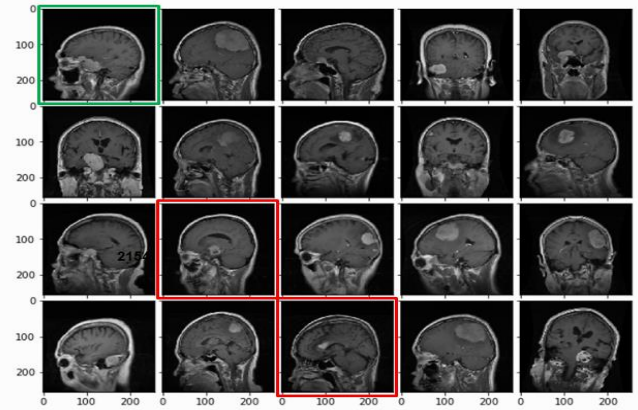
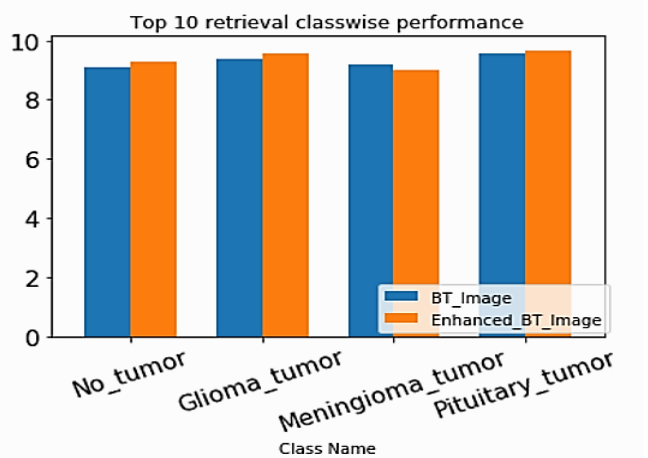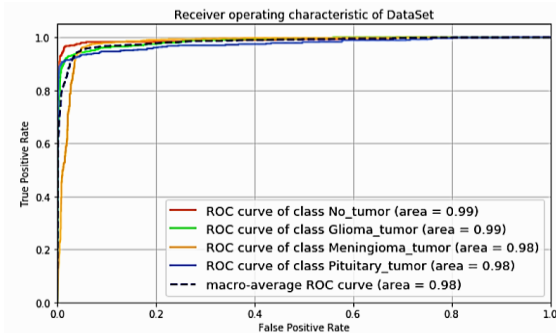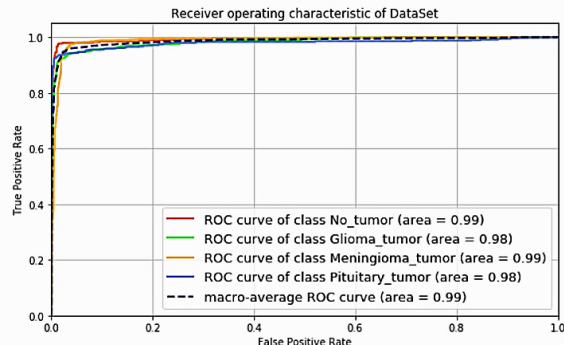**Figure 4.** Top 20 retrieved Brain tumor image for a query image

Figure 5. Class-specific retrieval of top 10 Brain tumor images

(a) ROC analysis using CBIR

(b) ROC analysis using SRE-CBIR

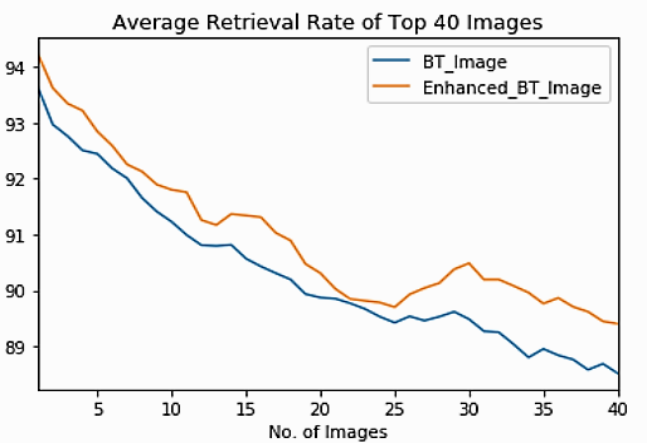**Figure 3.** ROC analysis of Brain tumor dataset

Figure 6. Retrieval rate of top 40 Brain tumor images

4.2 Results analysis of COVID19

Table 4 shows the results of the COVID19 dataset, the average precision using original COVID19 image is 97.0%, which is 98.0% using the enhanced COVID19 image. There is also a 1.2% increase in the weighted average precision with enhanced COVID19 image. The precision value is the same for Pneumonia cases i.e. 97% , whereas it is increased by 2% in the Covid-positive case and 1% in the Covid-negative case. The average recall rate is improved from 97.0% to 98.3% and the f1-score is increased from 97.0% to 97.7% using enhanced image dataset. Total 6498 images are analyzed and the number of images belonging to different classes are shown as the support value.

Table 4. Performance analysis of Covid19 dataset

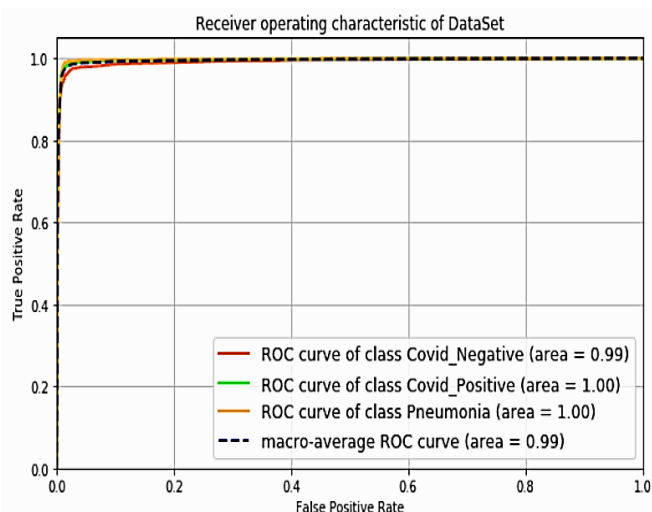|	Original Covid19 Image			Enhanced Covid19 Image			
	Precision	Recall	f1- Score	Precision	Recall	f1- Score	Support
Covid Negative	0.98	0.97	0.97	0.99	0.99	0.97	3024
Covid Positive	0.96	0.96	0.97	0.98	0.98	0.98	2531
Pneumonia	0.97	0.98	0.97	0.97	0.98	0.98	943
Macro Avg.	**0.970**	**0.970**	**0.970**	**0.980**	**0.983**	**0.977**	**6498**
Weighted Avg.	**0.971**	**0.968**	**0.970**	**0.983**	**0.985**	**0.975**	**6498**

Figure 7 shows the ROC curve of the original and the enhanced COVID19 image. The macro-average ROC is enhanced from 99% for the original dataset whereas it is 100% using the proposed enhanced dataset. Figure 8 presents the top 20 retrieved COVID19 images with respect to a query image. The query image is shown using a green border. Here all the images belong to the same class of the query image so there is no image with a red border. The class-specific retrieval performances of the top 10 COVID19 images are shown in Figure 9. The performances of all the classes except the Pneumonia class is comparatively enhanced using the proposed CBIR model. Figure 10 presents the average retrieval values of the top 40 COVID19 images. It indicates the value of average retrieval rate improves as more images are retrieved. Hence a better CNN feature is generated using the enhanced COVID19 images.
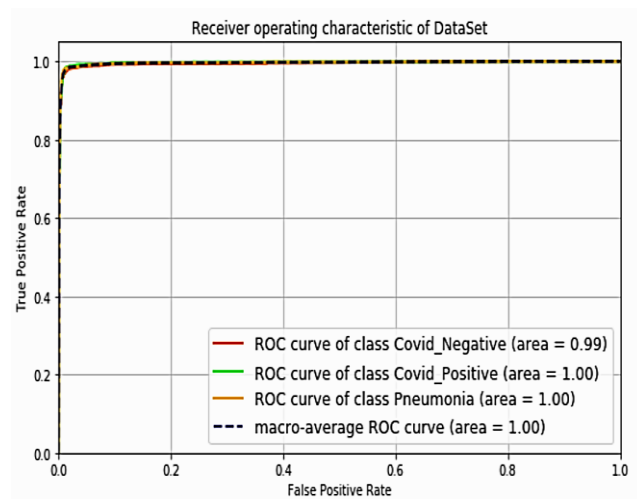
Table 5 shows the comparison of accuracy of Brain tumor and COVID19 datasets using deep-learning and other optimization techniques and the proposed saliency-region enhanced method.

Table 5. Comparison of proposed SRE-CBIR method performance with existing state-of-art

Sl. No.	Research Study/ Year	Method Used	Modality of Scan	Image Database	Accuracy
1	Horry et al. [11]	Deep Learning VGG19	Chest X-ray	COVID19	86%
2	Ismael et al. [16]	Deep Learning ResNet50 Features + SVM	Chest X-ray	COVID19	94.7%
3	Pathan et al. [20]	CNN hyperparameters are optimized using WOA-BAT optimization techniques	Chest CT-Scan	COVID19	96%
4	Panwar et al. [35]	Deep Learning nCOVnet	Chest X-ray	COVID19	97.62%
5	Deepak et al. [25]	Deep Learning pre-trained GoogLeNet	Brain tumor MRI scan	Brain MRI	94.7%
6	Proposed Method	Saliency enhanced CNN feature	Chest X-ray	COVID19	**98.00%.**
7	Proposed Method	Saliency enhanced CNN feature	Brain tumor MRI scan	Brain MRI	**95.00%**

(a) ROC analysis using CBIR

(b) ROC analysis using SRE-CBIR
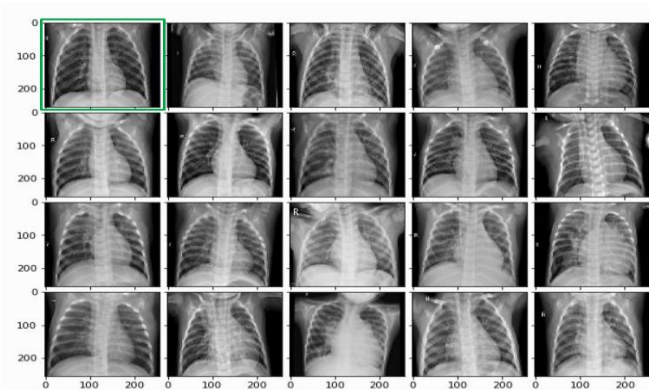
Figure 7. ROC analysis of COVID19 dataset

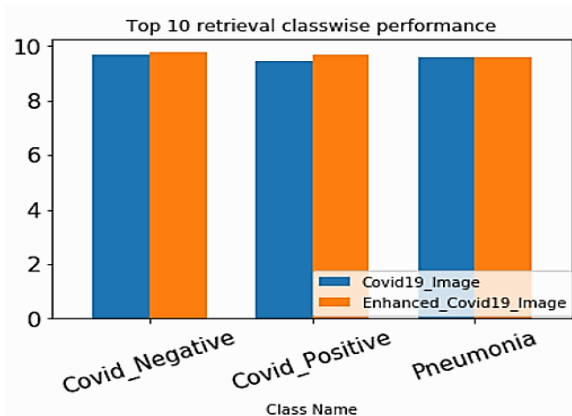**Figure 8.** Top 20 retrieved COVID19 image with respect to a query image

Figure 9. Class-specific retrieval of top 10 Covid19 images
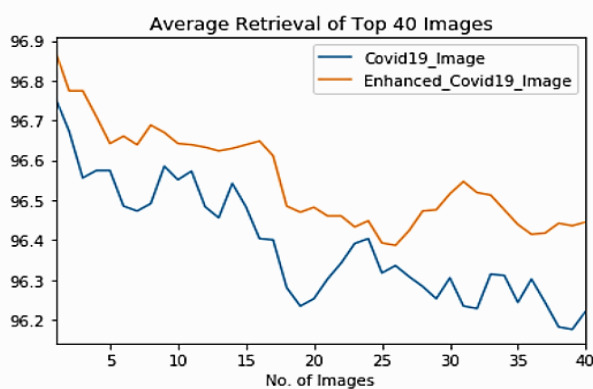

Figure 10. Retrieval rate of top 40 Covid19 images

5. CONCLUSIONS

This paper proposed a novel CBIR model for the medical image retrieval using CNN feature descriptor. Objective of this paper is to retain more RoA region information of the radiological image in the feature descriptor, identical to a doctor try to find the Region-of Attention area to analyze the image. To achieve the same initially the RoA area is segmented using U-Net, referred as mask-image. The mask-image is enhanced and fused with the original input image. The performance of the original radiological image CNN feature and the enhanced image CNN feature of the are tested using two datasets i.e. Brain tumor and COVID19 datasets. The retrieval results using the CNN features of the enhanced images show significant improvements for both the datasets. Moreover retrieval rate is improved as we retrieve more images from the dataset, it ascertains more class properties are retained using the enhanced image CNN feature. The enhancement in the f1-score implies these features are more stable to the class-imbalance issue. Further analysis can be done for other radiological images.

REFERENCES

[1] Ayesha, H., Iqbal, S., Tariq, M., Abrar, M., Sanaullah, M., Abbas, I., Rehman, A., Niazi, M.F.K., Hussain, S. (2021). Automatic medical image interpretation: State of the art and future directions. Pattern Recognition, 114: 107856. https://doi.org/10.1016/j.patcog.2021.107856

[2] Kim, J., Cai, W., Feng, D., Wu, H. (2006). A new way for multidimensional medical data management: Volume of interest (VOI)-based retrieval of medical images with visual and functional features. IEEE Transactions on Information Technology in Biomedicine, 10(3): 598-607. https://doi.org/10.1109/TITB.2006.872045

[3] Marchiori, A., Brodley, C., Dy, J., Pavlopoulou, C., Kak, A., Broderick, L., Aisen, A.M. (2001). CBIR for medical images-an evaluation trial. In Proceedings IEEE Workshop on Content-Based Access of Image and Video Libraries (CBAIVL 2001), pp. 89-93. https://doi.org/10.1109/IVL.2001.990861

[4] Pradhan, J., Kumar, S., Pal, A.K., Banka, H. (2018). A hierarchical CBIR framework using adaptive tetrolet transform and novel histograms from color and shape features. Digital Signal Processing, 82: 258-281. https://doi.org/10.1016/j.dsp.2018.07.016

[5] Devulapalli, S., Potti, A., Krishnan, R., Khan, M.S. (2021). Experimental evaluation of unsupervised image retrieval application using hybrid feature extraction by integrating deep learning and handcrafted techniques. Materials Today: Proceedings. https://doi.org/10.1016/j.matpr.2021.04.326

[6] Palai, C., Jena, P.K., Pattanaik, S.R., Panigrahi T., Mishra, T.K., (2023) Content-based image retrieval using encoder based rgb and texture feature fusion. (IJACSA) International Journal of Advanced Computer Science and Applications, 14(3): 28. https://doi.org/10.14569/IJACSA.2023.0140328

[7] Jena, P.K., Khuntia, B., Anand, R., Patnaik, S., Palai, C. (2020). Significance of texture feature in NIR face recognition. In 2020 First International Conference on Power, Control and Computing Technologies (ICPC2T), pp. 21-26. https://doi.org/10.1109/ICPC2T48082.2020.9071504

[8] Pang, S., Orgun, M.A., Yu, Z. (2018). A novel biomedical image indexing and retrieval system via deep preference learning. Computer Methods and Programs in Biomedicine, 158: 53-69. https://doi.org/10.1016/j.cmpb.2018.02.003

[9] Majhi, M., Pal, A.K., Islam, S.H., Khurram Khan, M. (2021). Secure content-based image retrieval using modified Euclidean distance for encrypted features. Transactions on Emerging Telecommunications Technologies, 32(2): e4013. https://doi.org/10.1002/ett.4013

[10] Palai, C., Jena, P.K., Khuntia, B., Mishra, T.K., Pattanaik, S.R. (2023). Content-based image retrieval using adaptive CIE color feature fusion. Revue d'Intelligence

Artificielle, 37(1): 63-72. https://doi.org/10.18280/ria.370109

[11] Horry, M.J., Chakraborty, S., Paul, M., Ulhaq, A., Pradhan, B., Saha, M., Shukla, N. (2020). COVID-19 detection through transfer learning using multimodal imaging data. IEEE Access, 8: 149808-149824. https://doi.org/10.1109/ACCESS.2020.3016780

[12] Kurian, P., Jeyakumar, V. (2020). Multimodality medical image retrieval using convolutional neural network. In Deep Learning Techniques for Biomedical and Health Informatics, pp. 53-95. https://doi.org/10.1016/B978-0-12-819061-6.00003-3

[13] Abbas, A., Abdelsamea, M.M., Gaber, M.M. (2021). Classification of COVID-19 in chest X-ray images using DeTraC deep convolutional neural network. Applied Intelligence, 51(2): 854-864. https://doi.org/10.1007/s10489-020-01829-7

[14] Al-Waisy, A.S., Al-Fahdawi, S., Mohammed, M.A., Abdulkareem, K.H., Mostafa, S.A., Maashi, M.S., Arif, M., Garcia-Zapirain, B. (2020). COVID-CheXNet: Hybrid deep learning framework for identifying COVID-19 virus in chest X-rays images. Soft Computing, 1-16. https://doi.org/10.1007/s00500-020-05424-3

[15] Chandra, T.B., Verma, K., Singh, B.K., Jain, D., Netam, S.S. (2021). Coronavirus disease (COVID-19) detection in chest X-ray images using majority voting based classifier ensemble. Expert Systems with Applications, 165: 113909. https://doi.org/10.1016/j.eswa.2020.113909

[16] Ismael, A.M., Şengür, A. (2021). Deep learning approaches for COVID-19 detection based on chest X-ray images. Expert Systems with Applications, 164: 114054. https://doi.org/10.1016/j.eswa.2020.114054

[17] Nayak, S.R., Nayak, D.R., Sinha, U., Arora, V., Pachori, R.B. (2021). Application of deep learning techniques for detection of COVID-19 cases using chest X-ray images: A comprehensive study. Biomedical Signal Processing and Control, 64: 102365. https://doi.org/10.1016/j.bspc.2020.102365

[18] Pathak, Y., Shukla, P.K., Tiwari, A., Stalin, S., Singh, S. (2020). Deep transfer learning based classification model for COVID-19 disease. Irbm, 43(2): 87-92. https://doi.org/10.1016/j.irbm.2020.05.003

[19] Hassantabar, S., Ahmadi, M., Sharifi, A. (2020). Diagnosis and detection of infected tissue of COVID-19 patients based on lung X-ray image using convolutional neural network approaches. Chaos, Solitons & Fractals, 140: 110170. https://doi.org/10.1016/j.chaos.2020.110170

[20] Pathan, S., Siddalingaswamy, P.C., Kumar, P., MM, M.P., Ali, T., Acharya, U.R. (2021). Novel ensemble of optimized CNN and dynamic selection techniques for accurate Covid-19 screening using chest CT images. Computers in Biology and Medicine, 137: 104835. https://doi.org/10.1016/j.compbiomed.2021.104835

[21] Saba, T., Mohamed, A.S., El-Affendi, M., Amin, J., Sharif, M. (2020). Brain tumor detection using fusion of hand crafted and deep learning features. Cognitive Systems Research, 59: 221-230. https://doi.org/10.1016/j.cogsys.2019.09.007

[22] Mudda, M., Manjunath, R., Krishnamurthy, N. (2022). Brain tumor classification using enhanced statistical texture features. IETE Journal of Research, 68(5): 3695-3706. https://doi.org/10.1080/03772063.2020.1775501

[23] Yu, H., Yang, L.T., Zhang, Q., Armstrong, D., Deen, M.J. (2021). Convolutional neural networks for medical image analysis: State-of-the-art, comparisons, improvement and perspectives. Neurocomputing, 444: 92-110. https://doi.org/10.1016/j.neucom.2020.04.157

[24] Ahuja, S., Panigrahi, B.K., Dey, N., Rajinikanth, V., Gandhi, T.K. (2021). Deep transfer learning-based automated detection of COVID-19 from lung CT scan slices. Applied Intelligence, 51: 571-585. https://doi.org/10.1007/s10489-020-01826-w

[25] Deepak, S., Ameer, P.M. (2019). Brain tumor classification using deep CNN features via transfer learning. Computers in Biology and Medicine, 111: 103345. https://doi.org/10.1016/j.compbiomed.2019.103345

[26] Mukkapati, N., Anbarasi, M.S. (2022). Brain tumor classification based on enhanced CNN model. Revue d'Intelligence Artificielle, 36(1): 125-130. https://doi.org/10.18280/ria.360114

[27] Pradhan, J., Pal, A.K., Banka, H., Dansena, P. (2021). Fusion of region based extracted features for instance- and class-based CBIR applications. Applied Soft Computing, 102: 107063. https://doi.org/10.1016/j.asoc.2020.107063

[28] Chen, C., Qin, C., Qiu, H., Tarroni, G., Duan, J., Bai, W., Rueckert, D. (2020). Deep learning for cardiac image segmentation: A review. Frontiers in Cardiovascular Medicine, 7: 25. https://doi.org/10.3389/fcvm.2020.00025

[29] Tzelepi, M., Tefas, A. (2018). Deep convolutional learning for content based image retrieval. Neurocomputing, 275: 2467-2478. https://doi.org/10.1016/j.neucom.2017.11.022

[30] Shakarami, A., Tarrah, H. (2020). An efficient image descriptor for image classification and CBIR. Optik, 214: 164833. https://doi.org/10.1016/j.ijleo.2020.164833

[31] Gkelios, S., Sophokleous, A., Plakias, S., Boutalis, Y., Chatzichristofis, S.A. (2021). Deep convolutional features for image retrieval. Expert Systems with Applications, 177: 114940. https://doi.org/10.1016/j.eswa.2021.114940

[32] Lai, Z., Deng, H. (2018). Medical image classification based on deep features extracted by deep model and statistic feature fusion with multilayer perceptron. Computational Intelligence and Neuroscience, 2018: 2061516. https://doi.org/10.1155/2018/2061516

[33] Öztürk, Ş. (2021). Class-driven content-based medical image retrieval using hash codes of deep features. Biomedical Signal Processing and Control, 68: 102601. https://doi.org/10.1016/j.bspc.2021.102601

[34] Alzu'bi, A., Amira, A., Ramzan, N. (2017). Content-based image retrieval with compact deep convolutional features. Neurocomputing, 249: 95-105. https://doi.org/10.1016/j.neucom.2017.03.072

[35] Panwar, H., Gupta, P.K., Siddiqui, M.K., Morales-Menendez, R., Singh, V. (2020). Application of deep learning for fast detection of COVID-19 in X-Rays using nCOVnet. Chaos, Solitons & Fractals, 138: 109944. https://doi.org/10.1016/j.chaos.2020.109944

[36] Quadri, R., Deshpande, A. (2022). Deep learning-based segmentation and classification of COVID-19 infection severity levels from CT scans. Revue d'Intelligence Artificielle, 36(1): 41-48. https://doi.org/10.18280/ria.360105

[37] Ahmed, M.Z., Mahesh, C. (2021). A weight based labeled classifier using machine learning technique for classification of medical data. Revue d'Intelligence Artificielle, 35(1): 39-46. https://doi.org/10.18280/ria.350104

[38] Aggarwal, M., Tiwari, A.K., Sarathi, M.P. (2022). Comparative analysis of deep learning models on brain tumor segmentation datasets: BraTS 2015-2020 datasets. Revue d'Intelligence Artificielle, 36(6): 863-871. https://doi.org/10.18280/ria.360606

[39] Jena, P.K., Khuntia, B., Palai, C., Nayak, M., Mishra, T. K., Mohanty, S.N. (2023). A novel approach for diabetic retinopathy screening using asymmetric deep learning features. Big Data and Cognitive Computing, 7(1): 25. https://doi.org/10.3390/bdcc7010025

[40] Vankayalapati, R., Muddana, A.L. (2021). Denoising of images using deep convolutional autoencoders for brain tumor classification. Revue d'Intelligence Artificielle, 35(6): 489-496. https://doi.org/10.18280/ria.350607